Spatially resolved fish population analysis for designing MPAs: influence on inside and neighbouring habitats

Asbjørn Christensen, Henrik Mosegaard, and Henrik Jensen

Christensen, A., Mosegaard, H., and Jensen, H. 2009. Spatially resolved fish population analysis for designing MPAs: influence on inside and neighbouring habitats. – ICES Journal of Marine Science, 66: 56–63.

The sandeel population analysis model (SPAM) is presented as a simulation tool for exploring the efficiency of Marine Protected Areas (MPAs) for sandeel stocks. SPAM simulates spatially resolved sandeel population distributions, based on a high-resolution map of all fishery-established sandbank habitats for settled sandeels, combined with a life-cycle model for survival, growth, and reproduction, and a three-dimensional hydrodynamic model for describing larval transport between the network of habitats. SPAM couples stock dynamics to ecosystem and anthropogenic forcing via well-defined drivers. The SPAM framework was tested using ICES statistical rectangle 37F2 as an MPA, and the impact on sandeel populations within the MPA and neighbouring habitats was investigated. Increased larval spillover compensated for lost catches inside the MPA. The temporal and spatial scales of stock response to MPAs demonstrated that ecosystem self-regulation must be included when modelling the efficiency of MPAs, and for lesser sandeel, that self-regulation partially counteracts the benefits of a fishing sanctuary. The use of realistic habitat connectivity is critical for both qualitative and quantitative MPA assessment. The results confirm that the stock levels are more sensitive to changes in life conditions of larval stages than later parts of the life cycle.

Keywords: life-cycle models, MPA networks, North Sea, population density effects, spatially resolved population dynamics.

Received 10 December 2007; accepted 28 June 2008; advance access publication 2 December 2008.

A. Christensen, H. Mosegaard and H. Jensen: DTU Aqua, National Institute of Aquatic Resources, Charlottenlund Slot, DK-2920 Charlottenlund, Denmark. Correspondence to A. Christensen: tel: +45 3396 3373; fax: +45 3396 3333; e-mail: asc@aqua.dtu.dk.

Introduction

Increasingly, Marine Protected Areas (MPAs) have become popular tools for the management of marine resources (Gerber *et al.*, 2003; Halpern, 2003). The techniques for designing MPAs are still under development, and the implementation of specific MPAs often rests on a sparse empirical basis, some of which is of anecdotal nature (Botsford *et al.*, 2003; Halpern, 2003). Modelling could therefore play an important role in challenging the internal consistency of the conceptual frameworks (Roberts *et al.*, 2003) that underlie current MPA planning, quantifying new or competing hypotheses and guiding future efforts towards optimal management of ecosystem resources. MPA-related modelling has emanated from two poles, bioeconomics and ecosystem research, with fisheries research in between. Traditionally, the two fields have had different perspectives: bioeconomists focus on harvest value, whereas ecologists also emphasize objectives such as biodiversity, recreational value, risk of species extinction, and protection from overfishing. In contrast, bioeconomists are often less optimistic (Armstrong, 2007) about the biological benefits of MPAs.

Ecologically, implemented MPAs have a positive effect on the target fauna: they “work” (Halpern, 2003). The results of the impact on fishing yield are mixed, which is usually attributed to the fact that the MPA effect on fishing yield depends on stock exploitation status before establishing the MPA (Gerber *et al.*, 2003). If fishing effort is beyond maximum sustainable yield (MSY), MPAs usually increase yield, because the ecosystem effect of an MPA is similar to an effort reduction (Botsford *et al.*, 2003).

Spatiality is an essential aspect of MPA modelling. Two-patch models (representing inside and outside the MPA) as prototype MPA situations have been studied extensively (Beverton and Holt, 1957; Gårdmark *et al.*, 2006; Kar and Matsuda, 2008), but it is difficult to relate patch model transport parameters (representing larval dispersal and adult migration between patches) and relative patch volumes (representing MPA size) to a real marine environment. Therefore, it is essential to apply realistic geometries and realistic propagule dispersal/stock migration to lend credibility to MPA modelling (Gaines *et al.*, 2003; Gerber *et al.*, 2003). Limited coastline MPAs are benign from a modelling perspective, because they are quasi-one-dimensional, allowing for systematic analysis and modelling. In a generic coastline model, Gaines *et al.* (2003) demonstrated the importance of reserve topology for the efficiency of an MPA, a feature that would be difficult to capture in two-patch models.

In the present study, a high-resolution habitat map is applied for realistic spatial representation, combined with a population model and state-of-art hydrodynamics for realistic propagule dispersal to investigate MPA overlapping with habitats of lesser sandeel (*Ammodytes marinus*) in the North Sea, particularly on the side effects on adjacent habitats. Lesser sandeel is very abundant in many shelf ecosystems, often playing a wasp-waist role (Rice, 1995) in the foodweb. The species is short-lived and non-migratory after juvenile settlement, which removes some uncertainties in quantifying the MPA efficiency. The most critical life stages are probably the larval stages (Wright and Bailey, 1996). In the North Sea, sandeel stocks are heavily exploited (ICES, 2007a) and have historically supported the largest industrial fishery. The relevance of North Sea sandeel stocks as MPA targets for precautionary management action has been emphasized by recent recruitment failures and subsequent fishery collapse, the underlying causes of which are still only hypothesized (ICES, 2007b).

Material and methods

Overview

The purpose of the sandeel population analysis model (SPAM) is to bridge the knowledge of underlying biological and hydrodynamic processes with population level dynamics. In this study, we propose that the influence of ecosystem and anthropogenic drivers can be expressed by three aggregated but well-defined key drivers (Figure 1).

(i) *A*: A sandeel larva-specific recruitment matrix that depends on origin and destination habitats and includes larval mortality and stock density effects. *A* can be expressed by elemental ecosystem processes, as shown below and partially computed from first principles.

(ii) *M*: Adult and juvenile mortality caused by direct ecosystem effects (predation, starvation, etc.) and other factors (e.g. age, disease, and pollution).

(iii) *F*: Fishing mortality (adult and juvenile). MPA efficiency is assessed by regulating *F*, corresponding to the MPA regulatory measures in question.

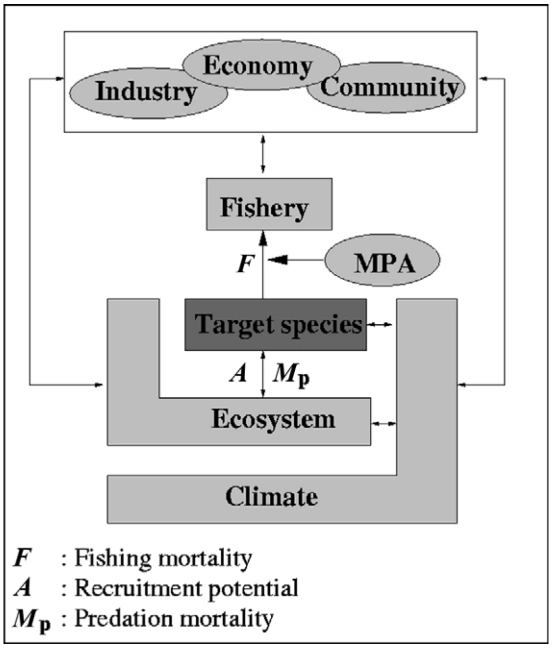

Figure 1. Target species in its ecosystem–socio-economic context. Arrows indicate causal relationships and interaction directions between components. The target species dynamics are decoupled via three aggregated driving forces (A, M_p, and F), with a clear definition in terms of underlying processes.

The model definition makes no *a priori* assumptions about spatial–temporal variability and complexity of the three key drivers. The three drivers constitute the essential interface of the North Sea sandeel stocks, as indicated in Figure 1. Because spatially resolved data for these drivers are currently lacking, temporal averages of the key drivers and spatial averages of M and F were applied as a first step towards understanding the stock response to MPAs. Starting with temporal averages is a useful (and necessary) first step towards building insight into the stock dynamics.

Scales and state variables

The state variables in the SPAM framework are the abundance N_{ia}^{y} and length L_{ia}^{y} resolved in space and time by regional and yearly indices (i, y), and on age cohorts a. The state variables describe regional averages at 1 January each year, so that they are "time snapshots" and not averages over the year. State variables are updated from 1 January to 1 January by integrating processes over the elapsed year. The model operates with two spatial resolution levels: a high-resolution level (10 × 10 km), where habitats and larval transport are described, and a regional-resolution level, within which state variables (N, L) are assumed constant. The model domain is formally the entire southern North Sea, but this study concentrates on the spatial region inside and around a test case MPA in ICES rectangle 37F2.

Process overview

The present framework is a life-cycle model for sandeels, which represents events affecting the reproductive value of each individual (directly or indirectly) at some level in the model. The main outcome is that the stock dynamic is described by the update

$$\begin{aligned} R_i^y &= \sum_{jb} A_{ijb}^y N_{jb}^y \\ N_{ia}^{y+1} &= R_i^y \delta_{a,0} \mathrm{e}^{-Z_{i0} t_{\mathrm{ps}}} + \mathrm{e}^{-Z_{ia-1}} N_{ia-1}^y \\ &= \sum_{jb} D_{iajb}^y N_{jb}^y, \end{aligned} \qquad (1)$$

with total yearly mortality $Z = F + M$. R refers to the recruitment referenced to settlement time (around May), $\delta_{a,0}$ is 1 for $a = 0$ and 0 otherwise, and t_{ps} is the post-settlement fraction of the year. Both A and D depend on N, and the model formulation is not bound to any particular regional division of small-scale habitats (sandbanks).

Process submodels

Habitats

The habitats of North Sea sandeels were mapped in detail recently by Jensen and Rolev (2004), based on a time-series of individual GPS-recorded fishing activities (Figure 2). From experimental studies and field investigations (Wright *et al.*, 2000), it is known that suitable sandeel habitats contain sandy sediment with minimal fine sediment fractions, to allow the fish to respire when buried in the seabed at night and during hibernation. The hydrographic requirements for suitable habitat are not as well characterized. Therefore, maps based on long time-series of fishing activities constitute the best current knowledge of the spatial distribution of potential habitats. The habitat quality cannot be resolved unambiguously from the fishery-based

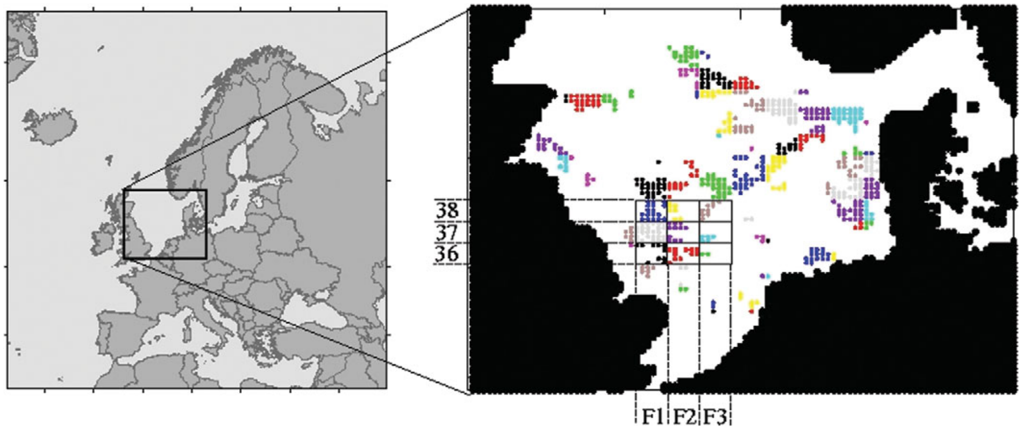

Figure 2. North Sea study area indicated by the square in the North Atlantic map, expanded to show North Sea sandeel habitats, grouped according to ICES statistical rectangle association, indicated by shadings. The target area of the MPA scenario simulation (ICES statistical rectangle 37F2) and the neighbouring ICES statistical rectangles containing sandeel habitats (ICES statistical rectangles 36F2, 38F2, 37F1, and 37F3) are shown by squares. Pixels represent hydrodynamic cell resolution for larval transport.

habitat map, so these maps were used only to *exclude* unsuitable areas.

The mapped habitat locations (fishing banks) were aggregated within each ICES statistical rectangle ($\sim$50 × 50 km), so that all habitats within an ICES statistical rectangle formed a habitat region with a habitat index in Equation (1). In total, this leads to 74 habitat regions in the southern and central North Sea (Figure 2). Habitats have not been graded relative to each other, apart from a carrying capacity, as discussed below.

Density effects

Density effects are mechanisms for stock self-regulation. If absolute stock abundance distribution is targeted, density effects must be included; otherwise, stock abundance generally explodes or vanishes, depending on the *per capita* reproductive number. For North Sea sandeels, population density effects may give rise to statistical significant abundance oscillations with a period of 2 years (Arnott and Ruxton, 2002) in the recruitment time-series. The precise mechanism has not yet been resolved, but plausible mechanisms are resource competition and/or cannibalism (of settled sandeels on eggs and larvae). Quantitatively, for larval cohorts, competition and cannibalism have a similar impact, so in this work, only food–shelter competition is highlighted, keeping in mind that the modelling efforts represent cannibalism to some extent as well. Larvae and adults feed on the same available zooplankton, although there is a weak tendency for larger sandeels to feed on larger food items (Macer, 1966). Because the zooplankton size spectrum is relatively constant on average, a common density index was used for both adults and larvae. The density index is considered representative for a growth season and evaluated at the beginning of a growth season. For a habitat region i at year y, the density index is

$$\rho_i^y = \frac{B_i^y}{C_i^y} = \frac{\sum_{a>0} N_{ia}^y w_{ia}^y}{C_i^y}, \tag{2}$$

where C_i^y and B_i^y are carrying capacity and biomass for habitat region i at year y, expressed via average weight per individual-at-age w_{ia}^y as elaborated below. For larvae transported between different regions (i and j), the average is used:

$$\rho_{ij}^y = \frac{1}{2}(\rho_i^y + \rho_j^y), \tag{3}$$

because a larva exchanged between regions i and j spends approximately (on average) equal time in regions i and j, and therefore the average experienced density factor corresponds to Equation (3).

Growth

A unified, continuous growth function was applied for larvae and adults. The average length L increment is represented as

$$\frac{\mathrm{d}L}{\mathrm{d}t} = \lambda(\rho)\left(\left(\frac{L}{L_\infty}\right)^{1-\beta} - \frac{L}{L_\infty}\right), \tag{4}$$

and integrated analytically over relevant growth periods for each cohort (in each habitat region). The growth periods for larvae, juveniles, and adults are t_{larv}, t_{juv}, and t_{agw}, respectively. The von Bertalanffy growth function is recovered for the special case $\beta = 1$. L_∞ is the estimated asymptotic length of *A. marinus* in the North Sea. For the 0-group in each region, the average length assigned is the abundance-weighted average of incoming and retained larvae, growing according to Equation (4). The growth envelope $\lambda(\rho)$ is parameterized as

$$\lambda(\rho) = \lambda_0 \frac{1+\rho}{1+\rho+2([\lambda_0/\lambda_1]-1)\rho^2}, \tag{5}$$

where λ_0 is the maximum growth potential at size, so that $0 < \rho < 1$ is the growth satiation regime, whereas $\rho > 1$ is the competition regime, where $\lambda \sim 1/\rho$ (caused by the factor ρ^2 in the denominator). We emphasize that our parameterization imposes the density effect on growth rate rather than on the asymptotic length L_∞, as advocated by Gårdmark *et al.* (2006). Gårdmark's approach would lead to occasional negative growth for adults in Equation (4), caused by fluctuations in ρ, unless Equation (4) is truncated for negative growth. Length is converted to weight using a constant allometric-scaling relationship (Macer, 1966):

$$w = w_\infty \left(\frac{L}{L_\infty}\right)^{\phi}. \tag{6}$$

Fishery yield Y

The biomass of the sandeel stock changes significantly during the growth season, and this was included by stipulating a representative catch day for the fishery season t_c, then integrating all cohorts forward using Equations (4) and (6), to obtain regional- and age-resolved fishery yields

$$Y^{y}_{ia} = N^{y}_{ia}(1 - e^{-F^{y}_{ia}})w^{y}_{ia}(t_c). \qquad (7).$$

Larva-specific recruitment A

The larva-specific recruitment is the number of surviving larvae per spawner at settlement (i.e. around May). Following the presettlement life path, recruitment at settlement time can be expressed as (Christensen *et al.*, 2008)

$$\begin{aligned} R_i &= \sum_{ja} (T^{y}_{ij} S^{y}_{ij} Q^{y}_{ja}) N^{y}_{ja} \\ &= \sum_{ja} A^{y}_{ija} N^{y}_{ja}, \end{aligned} \tag{8}$$

where T^{y}_{ij} is the hydrodynamic larval transport from region j to i at year y, S^{y}_{ij} the along-path survival chance (given successful transport), and Q^{y}_{ja} the (sex-averaged) age cohort a fecundity at region j for year y.

Fecundity Q

A model adapted from Macer (1966) is used:

$$Q_a = Q_\infty \left(\frac{L}{L_\infty}\right)^{q} \mu(a-2), \tag{9}$$

so spawning is restricted to the 2+ age groups [μ is the step function, with $\mu(x \geq 0) = 1$]. Spawning is formally assigned to 1 January after age promotion.

Larval transport T

Larval transport success T is a central component in MPA simulations, because it determines larval spillover and influx at the MPA boundary (i.e. habitat connectivity), as well as self-recruitment success. In previous work (Christensen *et al.*, 2007, 2008), T^{y}_{ij} was calculated from first principles and analysed in detail. In the present work, these high-resolution transport matrices were transformed to a regional division corresponding to ICES statistical rectangles (see Christensen *et al.*, 2008, for transformation procedure). Transport matrices T, averaged for the period 1999–2004, were entered in the matrices A in Equation (8). The averaged transport matrices captured the characteristic spatial transport patterns in the region, reflecting the goal of assessing the average long-term effect of MPAs, rather than a specific period in time.

Conditional (given transport) larval survival S

S is the product of predation avoidance (S_p) and starvation avoidance (S_s) probabilities. The former is parameterized simply as

$$S_p = e^{-M_{pl} t_{larv}}, \tag{10}$$

where t_{larv} is the larval planktonic phase with a constant North Sea average presettlement predation risk M_{pl}. For larvae, predation risk drops dramatically with size. Larval predation mortality was assumed to scale with larval mass as $w^{-1/4}$ (Sheldon *et al.*, 1972; Thygesen *et al.*, 2005), whereby the average predation risk for sandeel for the planktonic period can be estimated to 0.403 M_{ph}, where M_{ph} is predation risk at hatch time. For the starvation part, consistency between growth and starvation risk is emphasized. Studies of larval growth suggest that starvation occurs when growth is less than a certain fraction s, reported for many fish species to be around two-thirds of the maximum growth potential λ_0 at size (Letcher *et al.*, 1996). On the other hand, previous work (Christensen *et al.*, 2007) has estimated a characteristic relative growth variability σ, ~20% for North Sea sandeels. In this work, starvation is related to the fraction of larvae exhibiting growth below λ_0. The result is

$$S_s(\rho) = \frac{1}{2} + \frac{1}{2}\operatorname{erf}\left(\frac{1}{\sigma}\left(1 - s\frac{1 + \rho + 2([\lambda_0/\lambda_1] - 1)\rho^2}{1 + \rho}\right)\right), \tag{11}$$

where $\lambda_0 = \lambda(0)$ and $\lambda_1 = \lambda(1)$, and erf() is the standard error function.

Input, diagnostic variables, and biological parameters

Ecosystem mortality M and fishing mortality F

The ecosystem (non-anthropogenic) mortality is decomposed as $M = M_p + M_0$. The latter M_0 is the background mortality caused by age, disease, pollution, and starvation. M_p is the net predation component. For the 0-group, M is scaled by the post-settlement fraction of the year, t_{ps}, because mortality before settlement has been accounted for (see previous section). The mortality levels (M, F) are estimated from the operational North Sea 4M multispecies model (ICES, 2005) as North Sea averages (Table 1), with no spatial variability of M for the reference state (i.e. without MPA measures). MPA consequences are then explored by setting $F = 0$ within the MPA (and keeping fishing mortality unchanged elsewhere).

Carrying capacity C

The regional carrying capacities for the density indices in Equation (2) are estimated so that average catches for each region are reproduced as well as possible, subject to the prescribed average fishing mortality F, and subject to time-averaged hydrodynamic transport T, as described above. This procedure converges well in the study

Table 1. Reference level mortality components based on the 4M model simulations.

Mortality per year	**Age class**					
	0	**1**	**2**	**3**	**4**	**5+**
$M_p^{ref} + M_0$	$0.8/t_{ps}$	1.2	0.6	0.6	0.6	0.6
F^{ref}	$0.057/t_{ps}$	0.743	0.712	0.789	0.489	0.489

Table 2. Biological parameters in the SPAM model.

Parameter	Description	Value	Unit	Sensitivity χ_P [Equation (12)]	Source
M_{pl}	Drift phase larval base level mortality	$(365/5.7) \times 0.403$	year^{-1}	−17.9	Estimate, this work
S	Larval minimum growth factor	0.67	–	−1.99	Letcher *et al.* (1996)
L_0	Larval hatch length	6.3	mm	0.222	Jensen (2001)
L_∞	Adult length limit	218	mm	−6.10	Macer (1966)
β	Growth exponent	0.501	–	7.38	Jensen (2001) and Boulcott *et al.* (2007)
λ_0	Maximum growth prefactor	$1.2 \times \lambda_1$	mm year^{-1}	1.66	Estimate, this work
λ_1	Reference growth prefactor	1.0×1175	mm year^{-1}	4.17	Jensen (2001) and Boulcott *et al.* (2007)
σ	Growth variability	0.2	–	−0.448	Jensen (2001)
w_∞	Adult weight limit	31.94	g	−0.0302	Macer (1966)
φ	Weight–length exponent	3.068	–	1.14	Macer (1966)
Q_∞	Fecundity limit	12 556	eggs	4.52	Macer (1966)
q	Fecundity–length exponent	3.055	–	70.4	Macer (1966)
t_{larv}	Larval growth/drift period	8/52	Year	−16.8	Jensen (2001)
t_{juv}	Juvenile growth period	12/52	year	0.147	Jensen (2001)
t_{ps}	Post-settlement period	16/52	year	−2.19	Jensen (2001)
t_{agw}	Adult somatic growth period	$0.5 \times 20/52$	year	2.90	Jensen (2001)
d_{catch}	Median day in fishing season	135	Calendar day	Diagnostic	Jensen (2001)

area, but for a full North Sea application, thorough validation is needed.

Biological parameters

The reference set of biological parameters characterizing the North Sea *A. marinus* in the SPAM is displayed in Table 2, along with references to sources. This reference setting does not consider spatial variability in parameters; this is partially justified by the fact that this paper focuses simulations on a limited region in the North Sea. Only two "free parameters" were estimated in this work, λ_0 and $M_{pl} = (365/T_{surv}) \times 0.403$, where $T_{surv} = 5.7$ d is the expected larval lifetime at hatch. Fortunately, T_{surv} has a narrow meaningful range: $T_{surv} < 5.4$ d leads to stock extinction at many banks known to be populated, whereas $T_{surv} > 6.0$ d leads to unrealistic demographic self-regulation. For the demonstration simulation, $T_{surv} = 5.7$ d was chosen. A reference value of $\lambda_0/\lambda_1 = 1.2$ was used, which is in reasonable agreement with normal length-at-age variability (ICES, 2007a). Growth parameters β and λ_1 for the entire life cycle were fitted, based on Jensen (2001) and Macer (1966). Finally, the factor 0.5 in t_{agw} accounts for decreased somatic growth caused by gonad development.

Parameter linear sensitivity analysis

To elucidate biological as well as error sensitivity in the model, the relative linear sensitivity χ_p of the spawning-stock biomass (SSB) inside the MPA, SSB_{MPA}, to changes in relevant model parameters p is computed according to the dimensionless expression

$$\chi_P = \frac{P}{SSB_{MPA}} \frac{\partial(SSB_{MPA})}{\partial P}, \tag{12}$$

after biological systems have equilibrated following the MPA establishment. Linear sensitivities are displayed in Tables 2 and 3 for the bank-specific forcing (T, C, M, and F). Only the elements involving the MPA are displayed.

Table 3. Sensitivity [Equation (12)] of anthropogenic and ecosystem drivers directly involving the MPA region; χ_F is normalized by F_{MPA} in Table 1.

Driver	Sensitivity χ_P
F_{MPA}	−2.16
C_{MPA}	0.187
Larval transport retention ($T_{MPA,MPA}$)	−0.0320
Larval transport influx ($T_{MPA,*}$)	1.10
Larval transport outflux ($T_{*,j}$)	0.343

Initialization

Simulations are started by a spin-up phase, where the sandeel distribution approaches the statistical average distribution corresponding to the forcing and biological parameters described above. The spin-up technique, also used in three-dimensional hydrodynamic modelling, ensures that state variables (N, L) are internally relaxed when the MPA simulation starts, so that model results are independent of initial conditions of (N, L). Normally, a spin-up phase ~50 years is sufficient to relax the stock state (N, L). Owing to non-linearities, multiple limit cycles (or equilibriums) of (N, L) in Equation (1) are possible, but this has not been observed in the model setup with current parameters.

Results

As an MPA demonstration case, the fishery in ICES statistical rectangle 37F2 at Dogger Bank was closed, and the influence on sandeel stocks within the MPA and the adjacent habitat regions (ICES statistical rectangles 36F2, 38F2, 37F1, and 37F3; Figure 2) was investigated.

The regional stock response to the MPA above is illustrated in Figure 3. In this scenario, the system is equilibrated corresponding to fishing mortality $F = F^{ref}$ (Table 1) throughout the area before establishing the MPA. After establishing the MPA (set to year 0), $F = F^{ref}$ outside the MPA, and inside the MPA, $F^{MPA} = 0$. The

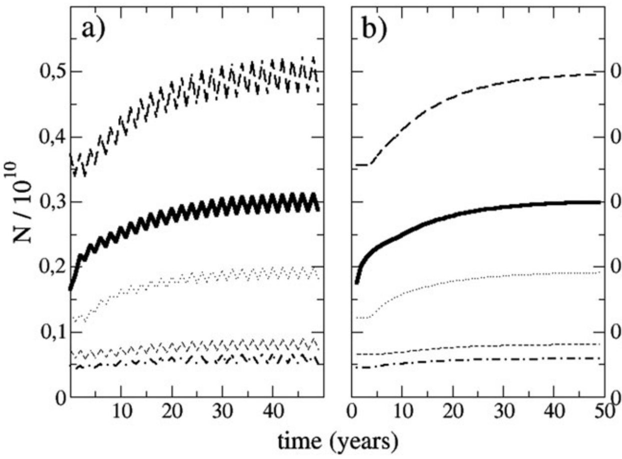

Figure 3. Stock dynamics in the MPA habitats (ICES statistical rectangle 37F2) and the neighbouring ICES statistical rectangles containing sandeel habitats (ICES statistical rectangles 36F2, 38F2, 37F1, and 37F3). *N* is the stock abundance of 1+ age groups in each habitat region. The MPA is closed to fishery at year 0 on the horizontal axis. Thick solid lines, 37F2; thin solid lines, 36F2; dotted lines, 38F2; broken lines, 37F1; long-broken lines, 37F3. (a) Stock abundance at 1 January each year after MPA establishment. (b) Stock abundance after MPA establishment smoothed over 2 years to enhance long-term trends.

value of *N* in Figure 3 at year 0 corresponds to the emergent stock size, when matching carrying capacity to reported landings in each ICES rectangle, as explained above. The population size varies with regular oscillations with a period of 2 years, consistent with Arnott and Ruxton (2002). The driving force for the oscillation is the resource competition between the 1-group and the settling 0-group, as mentioned above. A strong 1-group suppresses the 0-group, which then becomes a weak 1-group, which facilitates a strong 0-group, and so forth. There were significant regional differences in the amplitude of the density-driven stock fluctuation (Figure 3a). The phase of the density-driven oscillation with a period of 2 years is somewhat arbitrary; the MPA could just as well be established 1 year later, and the long-term response is unaffected by this. To emphasize the long-term trends (which are most relevant in the context of MPAs), model output (Figure 3a) was averaged over two subsequent years, thus filtering out the oscillations (Figure 3b). The sandeel stock within the MPA responded immediately to the effort closure, whereas the adjacent regions have a response lag of 2–3 years. This is basically caused by the fact that the influence of the MPA on adjacent regions is given by larval spillover from MPA. The MPA response time-scale, i.e. the time-scale for the MPA stock to re-equilibrate is ∼3 years, consistent with the sandeel maturation schedule. Adjacent regions are coupled to this time-scale, plus the time-scale to re-equilibrate their own age structures. These adjacent stocks also generate larval return spillover to the MPA, so the total response history for the MPA and adjacent regions becomes relatively prolonged, ∼6–10 years, before the effect of the effort closure has travelled through all state variables (N, L) describing the stock components. The response amplitudes of adjacent regions are also remarkably different; this relates to the patterns of ocean current for transport so adjacent regions receive different larval spillover from the MPA.

The long-term MPA effect on the local stocks is modest: a 10–50% stock increase, mostly in the MPA. A larger stock increase might have been expected following removal of the large mortality component (F) in the MPA. The main reason for the modest stock increase, apart from larval spillover, results from the dynamics of the density parameter ρ in the MPA and adjacent regions (Figure 4). In all areas, the resource competition level increases, most strongly within the MPA itself but also notably in adjacent areas. This increase in resource competition level partially compensates for the effect of reduced fishery effort. This result is a significant outcome of the modelling example and is a point also emphasized by Gårdmark *et al.* (2006) with a generic two-patch MPA model. They also noted that the total fishing-yield increase predicted for stocks exploited beyond MSY vanished if density effects were included in fish growth. The present model, which includes explicit habitat connectivity in addition to density effects on fish growth, gives a more positive prediction for the specific MPA test case considered in this work: the net local fishing yield (ICES statistical rectangles 37F2 and the neighbouring rectangles 36F2, 38F2, 37F1, and 37F3) is roughly unchanged, whereas the total southern North Sea yield *increases* by 16%. This is caused by larval spillover to more distant habitat regions, which cumulatively increase yield. When habitat regions are aggregated by neighbour shells (i.e. first, second, . . . neighbour group), all yield changes are positive, and the larval spillover influence distance is ∼100–150 km, although the convergence is not smooth with notable long-range interaction (Figure 5). The yield and SSB increase in neighbouring habitats is mostly slaved to SSB build-up within the MPA, rather than a propagating wave of biomass increase. Most of the recovery is completed within ∼10 years (Figure 5), but full recovery requires ∼30 years, consistent with Figure 3. The yield increase plot (Figure 5) displays a clear distance scaling, with important directional effects as indicated

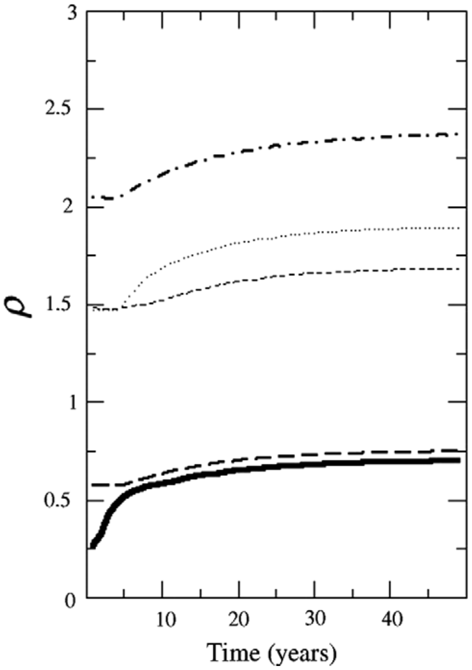

Figure 4. Dynamics of density index ρ in the MPA habitats (ICES statistical rectangle 37F2) and the neighbouring ICES statistical rectangles containing sandeel habitats (ICES statistical rectangles 36F2, 38F2, 37F1, and 37F3). Thick solid lines, 37F2; thin solid lines, 36F2; dotted lines, 38F2; broken lines, 37F1; long-broken lines, 37F3.

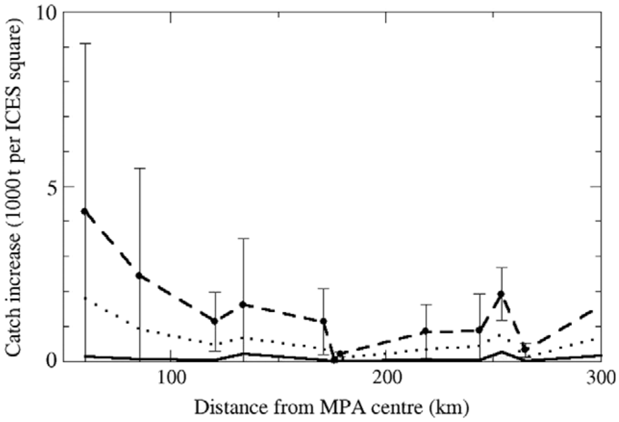

Figure 5. Catch increase per habital region (ICES square) per year plotted as a function of the distance from the MPA centre. Solid line, 4 years after MPA establishment; dotted line, 10 years after MPA establishment; broken line, 50 years after MPA establishment. Vertical bars on the broken line are the directional effect (root mean square on yield change on a given distance).

by the large variance (vertical bars), again reflecting that realistic spatial representation is necessary for quantitative predictions of MPA efficiency.

Discussion

The SPAM is a broad framework integrating first-principles hydrodynamic calculations, biological process knowledge, and fishery data. The current setup only models state variables (N, L) resolved by region and age class. However, often, the subscale and local variability of a state variable is interesting (and necessary) for matching observations and improving modelling from a process-orientated starting point. Currently, the state variable variance is only addressed at the recruitment phase at two points: first, the length distribution of new recruits at settlement time, which partly originate in other regions with other growth conditions, and second, at the competition-driven link between larval growth and survival. We believe that, for sandeels, the state variables (N, L) resolved by region and age describe the essential biology, but for more quantitative studies, it may be necessary to invoke auxiliary state variables, such as condition factors of cohorts, as well as explicit variance dynamics modelling.

The regional division in this work was based on ICES statistical rectangles, which are administrative rather than biological units. Often, ICES statistical rectangles artificially divide naturally connected habitats. Habitat mapping is a powerful tool for detailed analysis of ecosystem structure, and more research is needed to devise optimal regional habitat aggregations, specific to different species. This model framework is not restricted to a specific regional definition, because transport indices and other aspects can be consistently transformed to any desirable regional definition.

In this work, only the density effects in the specific recruitment index A have been considered, which we believe is most important, and in fecundity via growth regulation. However, the other stock dynamic drivers are also expected to display some dependence on sandeel density: F (e.g. fleet effort allocation, investment dynamics, etc.) and M_p (e.g. predator switching, predator attraction, vulnerability, and bottom–up regulation). Addressing these factors is beyond the scope of the present study. Omission of multispecies effects is a clear limitation in the current setup, but without better biological information, only crude assumptions can be used. Further, this study has not addressed regional variability in mortality components owing to lack of data. However, it is to be hoped that this and other studies will emphasize the importance of gaining more insight into this aspect in future survey programmes. Another spatial resolution issue is the reported regional fecundity variability for sandeels (Boulcott *et al.*, 2007). This regional variability may be a plastic response to environmental conditions, because genetic analysis did not provide evidence for different populations throughout the northern European shelf region (Wright *et al.*, 1998).

The regional carrying capacities (C_i) have been estimated in a rather preliminary approach, assuming that they match average local catches, using average transport indices and North Sea average efforts. This approach is being refined using time-resolved forcing to produce either time-resolved carrying capacities or improved representative average regional carrying capacities and to relate carrying capacities to habitat area and local zooplankton productivity. In this work, time-averaged ecosystem drivers (T, C, M_p) are applied to distil the effect of imposing the MPA rather than focusing on a specific year for MPA establishment. A future improvement is also to test the scope of natural time variability in the ecosystem drivers, because this may create a bias in modelled MPA impact, caused by non-linear responses. A systematic analysis of these aspects, beyond linear response to local driver variability in Table 3, is complex and beyond the scope of this paper, and involves spatial non-locality and driver interaction in the response.

Our results produced many testable hypotheses. The total southern North Sea yield increased by 16%, as a result of larval spillover to other regions, with a characteristic spillover range of 100 km. The precise magnitude of the stock self-compensation effect depended on crude parameterizations of important processes, but the compensation effect itself is always present. The compensation effect also provides an important prediction of the model: sandeel MPA measures should have a negative effect on sandeel growth. In support of this, sandeel growth appears to be slower in unexploited areas (Arnott and Ruxton, 2002). Real stock-abundance oscillations were also detected statistically in North Sea substocks by Arnott and Ruxton (2002); however, they are not as clear as in Figure 3, because they are disguised by assessment uncertainty and interannual variability in forcing, which is not addressed in this scenario simulation. Resource competition level may be very different in adjacent areas, even in the absence of MPA measures (Figure 4; time = 0). This may explain part of the observed growth variability in North Sea sandeel stocks.

Acknowledgements

This work has in part been supported by EU FP6/SSP projects BECAUSE (contract No. 502482), PROTECT (contract No. 513670), and the national DFFE/FIUF project "Fiskeriudsigt for tobis i Nordsøen på bankeniveau". Valuable and helpful advice from Morten Vinter on multispecies aspects and data of this work is greatly acknowledged.

References

Armstrong, C. W. 2007. A note on the ecological-economic modelling of marine reserves in fisheries. Ecological Economics, 62: 242–250.

Arnott, S. A., and Ruxton, G. D. 2002. Sandeel recruitment in the North Sea: demographic, climatic and trophic effects. Marine Ecology Progress Series, 238: 199–210.

Beverton, R. J. H., and Holt, S. J. 1957. On the Dynamics of Exploited Fish Populations. Fish and Fisheries Series 11. Chapman and Hall, London, UK.

Botsford, L. W., Micheli, F., and Hastings, A. 2003. Principles for the design of marine reserves. Ecological Applications, 13: S25–S31.

Boulcott, P., Wright, P. J., Gibb, F. M., Jensen, H., and Gibb, I. M. 2007. Regional variation in maturation of sandeels in the North Sea. ICES Journal of Marine Science, 64: 369–376.

Christensen, A., Daewel, U., Jensen, H., Mosegaard, H., St John, M., and Schrum, C. 2007. Hydrodynamic backtracking of fish larvae by individual-based modelling. Marine Ecology Progress Series, 347: 221–232.

Christensen, A., Jensen, H., Mosegaard, M., St John, M., and Schrum, C. 2008. Sandeel (*Ammodytes marinus*) larval transport patterns in North Sea from an individual-based hydrodynamic egg and larval model. Canadian Journal of Fisheries and Aquatic Sciences, 65: 1498–1511.

Gaines, S. D., Gaylord, B., and Largier, J. L. 2003. Avoiding current oversights in marine reserve design. Ecological Applications, 13: S32–S46.

Gårdmark, A., Jonzen, N., and Mangel, M. 2006. Density-dependent body growth reduces the potential of marine reserves to enhance yields. Journal of Applied Ecology, 43: 61–69.

Gerber, L. R., Botsford, L. W., Hastings, A., Possingham, H. P., Gaines, S. D., Palumbi, S. R., and Andelman, S. 2003. Population models for marine reserve design: a retrospective and prospective synthesis. Ecological Applications, 13: S47–S64.

Halpern, B. S. 2003. The impact of marine reserves: do reserves work and does reserve size matter? Ecological Applications, 13: S117–S137.

ICES. 2005. Report of the Study Group on Multispecies Assessment in the North Sea (SGMSNS), 5–8 April 2005, Copenhagen, Denmark. ICES Document CM 2005/D: 06. 159 pp.

ICES. 2007a. Report of the Working Group on the Assessment of Demersal Stocks in the North Sea and Skagerrak (WGNSSK), 5–14 September 2006, Copenhagen, Denmark. ICES Document CM 2005/ACFM: 35. 1160 pp.

ICES. 2007b. Report of the Study Group on Recruitment Variability in the North Sea Planktivorous Fish (SGRECVAP), 7–11 May 2007, Plymouth, UK. ICES Document CM 2007/LRC: 07. 69 pp.

Jensen, H. 2001. Settlement dynamics in the lesser sandeel (*Ammodytes marinus*) in the North Sea. PhD thesis, University of Aberdeen.

Jensen, H., and Rolev, A. M. 2004. The sandeel fishing grounds in the North Sea. Information about the foraging areas of the lesser sandeel (*Ammodytes marinus*) in the North Sea. Working document prepared for the BECAUSE project, November 2004.

Kar, T. K., and Matsuda, H. 2008. A bioeconomic model of a single-species fishery with a marine reserve. Journal of Environmental Management, 86: 171–180.

Letcher, B. H., Rice, J. A., Crowder, L. B., and Rose, K. A. 1996. Variability in survival of larval fish: disentangling components with a generalized individual-based model. Canadian Journal of Fisheries and Aquatic Sciences, 53: 787–801.

Macer, C. T. 1966. Sand eels (Ammodytidae) in the south-western North Sea; their biology and fishery. Fishery Investigations, 24 II: 6.

Rice, J. 1995. Food web theory, marine food webs, and what climate change may do to northern marine fish populations. *In* Climate Change and Northern Fish Populations, pp. 561–568. Ed. by R. J. Beamish. Canadian Special Publication of Fisheries and Aquatic Sciences, 121.

Roberts, C. M., Branch, G., Bustamante, R. H., Castilla, J. C., Dugan, J., Halpern, B. S., Lafferty, K. D., *et al.* 2003. Application of ecological criteria in selecting marine reserves and developing reserve networks. Ecological Applications, 13: S215–S228.

Sheldon, R. W., Sutcliffe, W. H., and Prakash, A. 1972. Size distribution of particles in the ocean. Limnology and Oceanography, 17: 327–340.

Thygesen, U. H., Farnsworth, K. D., Andersen, K. H., and Beyer, J. E. 2005. How optimal life history changes with the community size-spectrum. Proceedings of the Royal Society B – Biological Sciences, 272: 1323–1331.

Wright, P., Verspoor, E., Andersen, C., Donald, L., Kennedy, F., Mitchell, A., Munk, P., *et al.* 1998. Population structure in the lesser sandeel (*Ammodytes marinus*) and its implications for fishery–predator interactions. Final Report DG XIV No. 94/071, October 1998.

Wright, P. J., and Bailey, M. C. 1996. Timing of hatching in *Ammodytes marinus* from Shetland waters and its significance to early growth and survivorship. Marine Biology, 126: 143–152.

Wright, P. J., Jensen, H., and Tuck, I. 2000. The influence of sediment type on the distribution of the lesser sandeel, *Ammodytes marinus*. Journal of Sea Research, 44: 243–256.

doi:10.1093/icesjms/fsn191